Widén, Joakim; Wäckelgård, Ewa; Paatero, Jukka; Lund, Peter

Impacts of distributed photovoltaics on network voltages

Published in:
Electric Power Systems Research

DOI:
10.1016/j.epsr.2010.07.007

Published: 01/12/2010

Document Version
Peer reviewed version

Please cite the original version:
Widén, J., Wäckelgård, E., Paatero, J., & Lund, P. (2010). Impacts of distributed photovoltaics on network voltages: Stochastic simulations of three Swedish low-voltage distribution grids. Electric Power Systems Research, 80(12), 1562-1571. https://doi.org/10.1016/j.epsr.2010.07.007

Impacts of distributed photovoltaics on network voltages: stochastic simulations of three Swedish low-voltage distribution grids

Joakim Widén, Ewa Wäckelgård, Jukka Paatero, Peter Lund

This is a postprint of an article published in Electric Power Systems Research
Vol. 80:12, p. 1562-1571, 2010.
DOI: 10.1016/j.epsr.2010.07.007

http://www.journals.elsevier.com/electric-power-systems-research/

Impacts of distributed photovoltaics on network voltages: stochastic simulations of three Swedish low-voltage distribution grids

Joakim Widén[a,*], Ewa Wäckelgård[a], Jukka Paatero[b], Peter Lund[b]

[a] *Department of Engineering Sciences, The Ångström Laboratory, Uppsala University, P.O. Box 534, SE-751 21 Uppsala, Sweden*

[b] *Advanced Energy Systems, Helsinki University of Technology, P.O. Box 2200, FI-02015 HUT, Finland*

[*] Corresponding author. Tel.: +46 18 471 37 82. Fax: +46 18 50 01 31. E-mail address: joakim.widen@angstrom.uu.se

Abstract

The continuously increasing application of distributed photovoltaics (PV-DG) in residential areas around the world calls for detailed assessment of distribution grid impacts. Both photovoltaic generation and domestic electricity demand exhibit characteristic variations on short and long time scales and are to a large extent negatively correlated, especially at high latitudes. This paper presents a stochastic methodology for simulation of PV-DG impacts on low-voltage (LV) distribution grids, using detailed generation and demand models. The methodology is applied to case studies of power flow in three existing Swedish LV grids to determine load matching, voltage levels and network losses at different PV-DG penetration levels. All studied LV grids can handle significant amounts of PV-DG, up to the highest studied level of 5 kW_p PV per household. However, the benefits of PV-DG in terms of relative improvement of on-site reduction of demand, mitigated voltage drops and reduced losses were most significant at a penetration level of 1 kW_p PV per household.

Keywords: Distributed generation; Photovoltaics; Low voltage; Distribution grids; Power flow

1 Introduction

Integration of distributed photovoltaics (PV-DG) in middle-voltage (MV) and low-voltage (LV) grids is increasing in many countries around the world. In the IEA-PVPS countries, the installed peak power increased from around 500 MW to 7000 MW between years 2000 and 2007 [1]. This development has been mainly due to generous subsidy schemes, such as feed-in tariffs and investment support, most notably in Germany and Japan [2]. Most newly installed systems are grid-connected distributed systems and many of these are installed in residential areas at LV (0.4 kV) customers.

With a more extensive integration of PV-DG in residential areas, it is important to assure that power quality and end-user voltages are not negatively affected. A number of areas around the world with high densities of PV-DG are currently being monitored [3]. The main conclusion is that negative grid impacts are few; however, many of these systems were designed to meet high concentrations of generation. With a more widespread adoption of PV-DG, retrofitting into existing grids is a probable scenario.

In general, distributed generation affects power flows in distribution grids and has impacts on network voltage levels and losses [4]. On the positive side, on-site generation can serve the power demand locally and thereby mitigate voltage drops along distribution feeders. On the other hand, excess power injection may cause voltage rise at low-load situations. The potential benefits and allowable integration limits of distributed generation depend on the match to the local load, but also on grid topology, cable impedances and transformer operation. For PV-DG, the main challenge is the diurnal and annual variations in power output.

Simulations of PV-DG are often based on a worst-case methodology [5, 6]. In the worst-case approach, low-load and high-load events are treated separately to find extreme impacts on the distribution grid. Such static worst cases do not show the spectrum of impacts between the extreme values. For example, it does not tell how often overvoltages occur in different network nodes or how voltages or losses vary with fluctuations in demand and on-site generation. To capture these effects a stochastic approach that takes

regular and random variations into account is necessary. A probabilistic approach based on random generation of demand and production events with Monte-Carlo simulations is presented for LV grids by Conti and Raiti [7]. Another approach is to use stochastic generation of whole sequential demand and generation data series. Examples of the latter approach are presented by Paatero and Lund [8] and Thomson and Infield [9].

Results from previous studies suggest that a limited amount of PV generation can be integrated in residential MV and LV grids compared to the total domestic electricity demand as seen over the whole year. Thomson and Infield report a finite probability for overvoltages with 2160 W_p PV systems at 50 % of the households of a whole MV feeder with connected LV grids in the UK [9]. Paatero and Lund found no negative grid impacts with 1 kW_p systems at all households in an MV grid with connected LV grids reduced to single nodes, but clear overvoltages at 2 kW_p per household [8]. Viawan [6] reports limits of 1 kW_p per household for simplistic static simulations, although probabilistic simulations suggest larger systems could be integrated.

At moderately high latitudes the allowed system sizes of 1 kW_p per household produce around 1 MWh per year, which can be compared to standard Swedish figures for domestic electricity which typically vary from 1 to 5 MWh per year for household electricity demand in apartments (excluding electricity for common spaces and maintenance) and from 2 to 7 MWh per year for household electricity in detached houses [10]. Although there are methods to control overproduction and voltages [6, 11] there is a need to further investigate impacts of PV-DG in real LV grids to determine how often problems appear. This gives a basis for determining how often and to what extent regulation must be applied.

2 Aim of the study

In this paper a stochastic approach to realistic simulation of PV-DG in LV grids is presented and applied to three examples of existing residential LV grids in Sweden. The aim is to determine the impacts of PV-DG on load matching, losses and end-user voltage

levels and how these depend on variations in electricity demand and PV generation. As for high-latitude countries in general, PV-DG in Sweden is subject to large annual and diurnal variations in insolation [12] and has to meet a residential electricity demand that is negatively correlated to the insolation [13]. To determine PV-DG impacts and possible benefits, these variations and correlations have to be taken into account. The simulations aim to increase the knowledge of PV-DG at high latitudes, as few detailed studies at these locations have hitherto been performed.

In previous papers, a stochastic model for domestic power demand has been presented [14, 15], based on modelling from domestic time-use data [16]. In this paper the demand model is used together with modelled PV generation in detailed power-flow simulations. Compared to previous models used for PV-DG simulations, the demand model has a realistic basis in the empirical time-use data that it is based on and it has been validated in detail against measurements of domestic electricity demand. Another important feature is that the negative correlation between lighting demand and PV generation is preserved by using the same insolation data in both models [14]. This is especially important as lighting is the single largest end-use category in Swedish households [10].

As it is hard to define a 'standard' LV grid configuration, the studied grids were chosen from three distinctly different end-use segments of which they are thought to be representative. Thus, two urban LV grids, one designed for district heating loads and one designed for direct electric heating loads, and one rural LV grid designed for a mix of customers are simulated. PV penetration is varied between 1 and 3 kW_p per household for all grids to show the impacts of varying production levels. As an additional case, one of the urban grids is simulated with zero energy houses, equipped with 5 kW_p PV systems that produce as much as the households consume on average on an annual basis.

An important consideration is the time resolution of the simulations. Minute-resolution is suggested by Thomson and Infield [9], but for simulations with annual series and a large number of network nodes this degree of detail becomes computationally heavy. A previous study of the impacts of time averaging on data series has indicated that hourly

averages of demand and insolation are sufficient for estimating the probabilities for network voltages with a high accuracy [17]. The simulations in this paper are therefore based on annual data series with hourly time steps.

The study is limited to LV grids supplied by an MV/LV transformer substation. The voltage is assumed constant at the transformer and no variation in the MV grid is taken into account. This could lead to underestimation of voltage variations in cases where voltage variation in the MV grid is large. As Povlsen [5] has shown, voltage control in manually operated tap-changing transformers can limit PV further by boosting the voltage close to the upper limit at low-load situations. In any case, the simulations still show internal variation resulting from the characteristics of the LV grid and correspond to cases where voltage variations in the MV/LV connection point are small or controlled at a close-to-constant level.

The applied methodology for demand and PV system modelling and an outline of power-flow simulation are described in Section 3. Section 4 presents the specific demand and generation data and the LV grid models used in the simulated cases. In Section 5 the results are presented and a concluding discussion is given in Section 6.

3 Methodology

To produce detailed and realistic data on voltage fluctuations in LV grids the ambition in this study has been to simulate specific hourly demand and generation data series for each individual end-user connection over a whole year. Power-flow simulations can then be performed to yield the voltage level at each end-user and at each interconnecting bus in the grid. A flowchart showing the simulation procedure is provided in Figure 1. Irradiation data, giving the beam and diffuse radiation components I_b and I_d in every time step k, are fed into a model for calculating the separate outputs P_g of a desired number of PV systems. The irradiation data are also used in a load model, after conversion into daylighting data L, used for calculating lighting demand. This makes sure that a negative correlation between PV generation and lighting is taken into account.

The load model yields total domestic active and reactive power demand data P_d and Q_d for each household j out of a total desired number of households. Demand and PV system output data are then assigned to the nodes of an LV grid model and the power flow in the grid is calculated, yielding the voltage V at each node n in every time step. The specific parts of the simulation process are described in more detail below.

3.1 Load modelling

The applied stochastic load model has been extensively described and validated in refs. [14, 15]. In the model, load profiles are generated for individual households in a bottom-up approach. The behaviour of individual household members is modelled through generation of synthetic activity sequences with a non-homogeneous Markov-chain process. The parameters of the Markov chain are hourly averaged transition probabilities for switching between activities, estimated from a large set of Swedish time-use data. The activities covered by the model include the main electricity-dependent activities in households, such as cooking, washing, watching TV, etc. Each activity is connected to a specified end-use load. Lighting demand is modelled from when people are at home and awake and depends on the daylight level, calculated from irradiation data with well-established conversion models. The stochastic generation of activity sequences causes a highly realistic spread of loads over time in each individual household's demand.

The model discriminates between weekdays and weekend days and between the demand of detached houses and apartments. It covers *household electricity*, i.e., it does not include electric space heating or domestic hot water heating. Reactive power demand depends on the end-use and is calculated from active-to-reactive power signatures reported in ref. [18]. Important characteristic features of real demand, such as demand diversity, regular variations over the day and the year, coincident behaviour and short time-scale fluctuations, are realistically reproduced [14]. The output of the model is individual end-use specific power demand data for a desired number of households during an arbitrary time period with a time-step length down to one minute. For more details on the load model, see refs. [14, 15].

3.2 PV system modelling

The applied PV system model calculates the power output from an arbitrarily oriented and sized system with standard components. From incident beam and diffuse radiation onto the horizontal plane the global incident radiation I on an arbitrarily oriented plane can be calculated. Standard transposition models, outlined in ref. [19] are used. From the global radiation in the plane of the PV array, the PV system output is calculated as

$$P_g = A_c I \eta_{mp} \eta_a \tag{1}$$

where A_c is the area of the photovoltaic array, η_{mp} is the maximum-power-point (MPP) efficiency of the solar cells and η_a is the efficiency of additional equipment (cables and inverters), including additional losses in the solar cells. While η_a is assumed constant, η_{mp} is temperature-dependent and can be described as [19]:

$$\eta_{mp} = \eta_{STC} \left[1 + \mu \left(T_a - T_{c,STC} + I \frac{T_{c,NOCT} - T_{a,NOCT}}{I_{NOCT}} (1 - \eta_{STC}) \right) \right] \tag{2}$$

where η_{STC} is the conversion efficiency at standard test conditions (STC), μ is the temperature coefficient of the conversion efficiency, $T_{c,STC}$ is the cell temperature at STC and $T_{c,NOCT}$, $T_{a,NOCT}$ and I_{NOCT} are the nominal operating cell temperature (NOCT) and the associated ambient temperature and incident radiation. Given a measured module size A_{ref} and an output P_{STC} at STC of this module, the reference conversion efficiency is

$$\eta_{STC} = \frac{P_{STC}}{I_{STC} A_{ref}} \tag{3}$$

where I_{STC} is the incident radiation at STC. The applied parameter values are shown in Table 1.

System size is expressed in terms of peak power at STC. The system peak power is

$$\widehat{P}_g = I_{STC} A_c \eta_{STC} = P_{STC} \frac{A_c}{A_{ref}} \tag{4}$$

and the normalised system output is

$$P_{norm} = \frac{P_g}{\widehat{P}_g} \tag{5}$$

The output from a system of any other dimension can be determined by multiplying the normalised output by the desired peak power.

3.3 Power-flow simulation

Newton's method [20] is applied to numerically calculate the three-phase balanced power flow in an LV distribution grid. A Matlab [21] script for simulation of an LV grid with specified cable impedances, loads and generation units was implemented and validated against known power-flow solutions. Power-flow simulations require a so-called 'slack node' to be defined as a constraint [20]. At the MV/LV substation node a constant 0.4 kV voltage is thus assumed and the power flow into the LV grid is unconstrained. As a consequence, voltage variation in the MV grid is not taken into account. The power-flow solution is the set of voltages at each end-use bus and each interconnecting bus in the network in each time step. From these voltages, line currents are determined and from these the losses in the cables can be calculated.

4 Simulation setups

One annual simulation with an hourly resolution was performed for each grid, which means that 8760 individual power flow solutions per grid were calculated. The setups of

the simulations are described below.

4.1 LV grid models

Data for three LV grids in the Uppsala region, Sweden, were obtained from Vattenfall Eldistribution AB. The obtained data include cable impedances and lengths of individual cables, interconnected buses and end-user connections. An overview of some properties of the grids is provided in Table 2. Two of the grids (A and B) are located in residential urban areas, one designed for serving district-heated houses and one designed for households with direct electric heating. The third grid (C) is located in a rural area. The grids serve different numbers of end-users. Grid A has the largest number of customers and grid C the smallest.

An overview of the grid topologies is provided in Figure 2. End-user cables are not shown in the figure, but the number of end-users connected to each bus is indicated. Each grid is served by an MV/LV transformer substation. Grid A consists mainly of linearly connected feeders, while grid B has a whole section that is looped. Grid C consists of a few relatively long feeders but with few connected customers. All cables have capacities well above the power flow ranges of all simulation cases. The MV/LV transformer ratings are not known, but if 800 kVA transformers are assumed, all studied power flows are handled.

4.2 Irradiation data

Measured irradiance data for Stockholm, Sweden (59° N, 18° E), were obtained from the Swedish Meteorological and Hydrological Institute (SMHI). Out of the total data available, covering more than 20 years, data from the year 1999 were chosen for the simulations. As seen over the available data range, this year appears to be representative in terms of total annual insolation [22]. The data series cover beam and diffuse radiation onto a horizontal plane for one year with an hourly resolution. SMHI temperature data

collected from a nearby station provide input to the calculations of the temperature dependence of the solar cells.

4.3 Demand and PV generation data

Individual annual series of electricity demand data with hourly time steps were generated with the demand model for every household in the respective grid. All houses were considered to be detached houses, simulated with the same household appliance parameters as in refs. [14, 15], yielding data that correspond closely to a representative measured sample of the Swedish population. The same distribution of household sizes as in [14, 15] was used, corresponding to the general distribution in the Swedish population. The demand of each household differs, mainly because of the variation in household sizes. The distribution of annual demand for different households in the grids is shown in Table 3. Mean values, maxima and minima differ since the demands are stochastically generated.

Identical PV systems are simulated for every household, which means that the penetration level in terms of households with installed systems is set to 100 %. As the systems are identical, aggregate generation profiles of several systems will differ only by a scaling factor. This is a reasonable assumption, as all systems will experience very similar or identical meteorological conditions when they are confined within a limited area, which can be assumed for the studied LV grids. Each system is oriented due south with a tilt of 45°, yielding a maximised annual production at the specific latitude. Penetration levels in terms of system sizes are varied in four different scenarios for every grid; 0, 1, 2 and 3 kW_p per household. An additional scenario with zero-energy houses was also run for grid A. In this case the PV system size was set to 5 kW_p per household, which gives an annual production roughly equal to the mean demand per household and year. Scenarios for the PV system sizes with annual production per system are shown in Table 4. A comparison with Table 3 shows that annual production in all but the highest PV generation scenario far from corresponds to the annual mean demand in the grids.

5 Results

5.1 General load matching

The degree of matching of on-site generation to the local demand determines the amount of imported and exported power from individual households and, in effect, the direction of power flows in the grid. In general, matching exhibits a higher degree of randomness for individual households than for larger numbers of households due to random load coincidence.

Mean hourly demand and PV generation profiles, averaged over a summer and a winter half-year period, are shown for grid A in Figure 3. As data for the other grids are generated with the same model, profiles for these are close to identical. There is a clear seasonal effect on the appearance of the daily profiles. The main effect on the load is the reduced peak demand in the summer, due to decreased need for lighting. There is also a small decrease in the morning for the same reason. At the same time the PV production is higher during summer, providing to the negative correlation between demand and generation.

The effects of varying PV system sizes are also seen in the figure. At the lowest PV penetration level the average maximum production is at the same level as the daytime demand during summer, while there is a more extensive summertime overproduction in the other cases. Still, the annual production at the highest penetration level corresponds only to little more than half of the annual demand.

Figure 4 shows the daily demand and PV generation on every day of the year, averaged over all households in grid A. There is a slight seasonal fluctuation in demand mainly due to lighting, and a more frequent fluctuation between roughly two values, corresponding to weekday and weekend day demand. The seasonal fluctuation in PV generation is evident and it is also clear that the variations between separate days are higher and more random than the demand variations. At the lowest penetration level, daily generation is much lower than the daily demand in the grid. At the highest penetration level, the daily

generation exceeds the demand for most days during summertime.

5.2 Local consumption and reverse flow

An important issue is how self-sufficient the simulated area is concerning on-site generated electricity. Overproduced power that is not met by demand in the grid results in reverse power flow through the substation transformer. As suggested by the variability in load matching over the year, this will vary with season.

Table 5 shows how often reverse flow occurs in average for different months and in relation to the total time with PV generation. At the 1 kW_p penetration level power flow is reversed on average a few hours per day during summer. For higher penetration levels there is reverse flow during a major proportion of the hours with PV; for example in June the power flow is reversed almost half of the time with PV generation. It should be noted that for many of the hours with PV generation the insolation is very low; under less ideal conditions the hours with production would be much fewer and the fraction of time with reverse flow higher.

Thus, at higher penetration levels a substantial proportion of the generated power is exported from the LV grid. Figure 5 shows in more detail the aggregate flows into and out of the three grids, including losses in the LV grid cables. The pattern is roughly the same for all households but with different magnitudes and slightly different proportions of losses. The figures on the left show that the energy imported into the LV grid is reduced substantially in the 1 kW_p case, but marginally less in the other cases; increasing the penetration level from 2 to 3 kW_p has virtually no effect on local demand reduction. Thus, PV generation above the 1 kW_p level successively increases the total energy flowing through the grid. As shown in the figures on the right in Figure 5, a minor fraction of the total injected power is exported through reverse flow at the 1 kW_p penetration level. At higher penetration levels, however, most generated electricity above that in the 1 kW_p case is exported. PV has an impact on losses, although the losses are small compared to the total power flow in the grid and hardly distinguishable from Figure 5. Network losses

are shown in Table 6. There is a marked decrease for the 1 kW_p case, then an increase with higher penetration levels as the total power flow in the grid increases.

5.3 Effects on voltage

As mentioned in the introduction, excess generation that is injected into the LV grid causes the voltage to rise. Ultimately, there is a possibility that the voltage at customers exceeds prescribed limits. These vary between different European countries with the largest allowed variations typically ±10 % within nominal voltage and the lowest around ±5 % within nominal voltage [23]. Design limits of grid companies when planning grids are typically ±5 % [24].

Per-unit voltage spans in the grids at different penetration levels are shown in Table 7. There is by default a voltage drop in the grids and voltage rise from PV that increases with increasing penetration level. The voltage spans are different for the different grids, with grid A having the largest variations and grid C the smallest. No voltage variations exceed the prescribed limits for any of the studied penetration levels. It is also clearly seen that the worst voltage drop is not mitigated by PV.

The distribution of voltages within these limits are shown in Figure 6, which shows the cumulative probability distribution for end-user voltages calculated over all household nodes and over the whole year. The curves show the probability for voltages below the indicated voltage level. Ideally, the voltage should be close to nominal for all households, which means the cumulative probability should be a step function going from 0 to 1 at the p.u. voltage 1. For the 0 kW_p base cases, the curves have a tail to the left corresponding to voltage drops. If PV-DG is able to counteract voltage drops it should shift the probability distribution towards the nominal voltage. This actually happens for the 1 kW_p penetration level, although the worst drops are unaffected and the probability for voltages higher than nominal also increases, as seen most clearly for grid A. With higher penetration levels, the improvement is smaller while there is mainly an increase of the probability for higher voltages. The impact is smaller for the other grids but follows

the same pattern.

It is important to note that not all households are equally affected by the voltage variations, since the voltage drops and rises at a customer site depend on the location in the grid. The temporal variations in demand and generation also imply that the hours of the year are unequally affected by voltage variations. Table 8 shows the total time over the whole year with at least one end-user experiencing a voltage above an indicated level. Table 9 shows the proportion of end-users with voltages above an indicated level at least once during the whole annual simulation period. These tables show that many households are not affected by voltage variations at all (except for the most extreme penetration level) and that voltage variations above the indicated limits occur during a limited time as seen over the whole year.

Figure 7 shows seasonal variations in the distribution of end-user voltages in grid A. Mean voltage and standard deviation together with minimum and maximum voltage among all end-users are shown for each month separately. The mean winter voltages remain virtually the same regardless of penetration level. The mean summer voltages increase with penetration level, as well as the voltage variation as indicated by the standard deviation and maxima. The minimum voltage is affected somewhat during summer but not during the rest of the year. Note that the worst-case voltage does not occur during summer but during spring. This is because of the PV panel tilt of 45°. While it maximises annual production the incidence angle of the noon-time sun to the normal of the PV array is smallest in spring and autumn. Consequently, the highest powers occur during spring and autumn although total production is highest in the summer.

5.4 Impacts of zero-energy houses

Cumulative probability for the end-user voltage in grid A with zero-energy houses is shown in Figure 8. There is a pronounced effect of the same type as for the lower PV penetration scenarios. The upper limit of 10 % is far from violated, but the 5 % limit is exceeded, however with a very low probability. Even this massive concentration of

generation is manageable in the weakest LV grid.

Figure 9 shows a summary of the total power flow in and out of the LV grid with the zero-energy house scenario. Unsurprisingly, this is also a continuation of the trend seen for the smaller PV system sizes. Demand and PV generation are equal, but most PV generation is exported to the MV grid through reverse flow while most of the demand is covered by import from the MV grid. The demand-to-export and generation-to-import proportions are not very far from a hypothetical worst case with totally unmatched demand and production, in which all demanded power is imported and all locally generated power is exported.

6 Concluding discussion

The stochastic approach presented in this paper gives a realistic description of the diversity and spread of impacts from PV-DG in LV grids. In contrast to worst-case simulations or simplified load models with poorly reproduced negative or positive correlations between production and demand data, it yields detailed information about the variation of voltage levels in simulated grids over days and seasons.

The case studies of PV-DG in the three Swedish LV grids show that PV-DG has a characteristic effect on grid voltages. The grid in the district-heated area (A) shows the largest voltage variations, and is the grid where voltage rises over certain levels occur most often and where the largest fractions of end-users are affected by voltage rises. However, no violations of prescribed voltage limits occur for any grid in any of the 1–3 kW_p cases. In the case with zero-energy houses the 5 % limit is exceeded with a small but finite probability, but the 10 % level is far from violated.

This is partly because the grids are relatively strong in order to take electric heating loads, which is also why the mainly district-heated area grid is the weakest. Possibly the voltage spans would be different if variations in the MV grid were taken into account and if tap-changing regulation raised the voltage at the MV/LV transformer to counteract the

(still relatively small) voltage drop. In particular, a larger variation would be expected for the rural grid, where MV cables span across longer distances. As mentioned in the introduction, these exact simulations hold for situations where there is little voltage variation at the MV/LV transformer substations, either because of the MV grid properties or through voltage control. It is also possible to conclude that for these grid examples, internal voltage rise in the LV grid will not be the limiting factor for PV-DG integration.

Anyway, the relative impact of PV should be the same, and even more pronounced, for grids with larger voltage variations if demand and production per household are the same. These impacts include: (a) small mitigation of voltage drops at 1 kW_p PV per household but no further improvement for higher penetration levels, (b) mainly increased probability for higher voltages and increased voltage variability because of poor matching above 1 kW_p per household, (c) reduction of losses at 1 kW_p per household and successive increase with higher penetration levels and (d) substantial reverse power flow through the MV/LV transformer supplying the grid at higher penetration levels.

None of these impacts present a definite limit for the PV penetration level. Instead, the role and purpose of PV is the main difference between the penetration-level scenarios. At 1 kW_p per household, almost all produced PV electricity is consumed internally in the LV grid, while it helps to reduce losses. At higher penetration levels the households are to a higher degree producers than consumers of their own PV production, as a substantial proportion is exported from the LV grid. In fact, the zero-energy houses are plus-energy houses for the vast majority of all produced electricity. The benefits of such massive integration in several LV grids cannot be determined without considering the surrounding and overlying grid levels and requires further analysis.

Acknowledgement

The work has been carried out under the auspices of The Energy Systems Programme, which is primarily financed by the Swedish Energy Agency. Alf Svärd and Peter Johansson at Vattenfall Eldistribution AB are gratefully acknowledged for providing data

for the LV grid models.

References

[1] IEA-PVPS, Trends in photovoltaic applications: survey report of selected IEA countries between 1992 and 2007. Report IEA PVPS T1-17:2008. Available from: http://www.iea-pvps.org/products/download/rep1_17.pdf (accessed 2009-05-03).

[2] IEA-PVPS, Annual report 2007. Implementing agreement on photovoltaic power systems. Available from: http://www.iea-pvps.org/ar/ar07/index.htm (accessed 2009-05-03).

[3] IEA-PVPS, Community-scale solar photovoltaics: housing and public development examples. Report IEA PVPS T10-04:2008.

[4] N. Jenkins, R. Allan, P. Crossley, D. Kirschen, G. Strobac, Embedded Generation, IET Power and Energy Series 31, 2000.

[5] A.F. Povlsen, Impacts of power penetration from photovoltaic power systems in distribution networks. Report IEA PVPS T5-10:2002.

[6] F.A. Viawan, Steady state operation and control of power distribution systems in the presence of distributed generation. Licentiate Thesis, Department of Electric Power Engineering, Chalmers University of Technology, Sweden.

[7] S. Conti, S. Raiti, Probabilistic load flow using Monte Carlo techniques for distribution networks with photovoltaic generators, Solar Energy 81 (2007) 1473–1481.

[8] J.V. Paatero, P.D. Lund, Effects of large-scale photovoltaic power integration on electricity distribution networks, Renewable Energy 32 (2007) 216–234.

[9] M. Thomson, D.G. Infield, Impact of widespread photovoltaics on distribution systems, IET Renewable Power Generation 1 (2007) 33–40.

[10] Swedish Energy Agency, Energy in Sweden 2008. ET2008:16. Available from: http://www.swedishenergyagency.se.

[11] J.D. Crabtree, Y. Dickson, L. Kerford, A. Wright, Methods to accomodate embedded generation without degrading network voltage regulation. EA Technology, 2001.

[12] B. Perers, The solar resource in cold climates. In: Ross, M., Royer, J. (Eds.), Photovoltaics in Cold Climates. James & James (Science Publishers) Ltd, London, 1999, pp. 20-29.

[13] J. Widén, E. Wäckelgård, P. Lund, Options for improving the load-matching capability of distributed photovoltaics at high latitudes, Solar Energy 83 (2009) 1953-1966.

[14] J. Widén, A. Nilsson, E. Wäckelgård, A combined Markov-chain and bottom-up approach to modelling of domestic lighting demand, Energy and Buildings 41 (2009) 1001-1012.

[15] J. Widén, E. Wäckelgård, A high-resolution stochastic model of domestic activity patterns and electricity demand, Applied Energy 87 (2010) 1880-1892.

[16] J. Widén, M. Lundh, I. Vassileva, E. Dahlquist, K. Ellegård, E. Wäckelgård, Constructing load profiles for household electricity and hot water from time-use data–Modelling approach and validation, Energy and Buildings 41 (2009) 753–768.

[17] J. Widén, E. Wäckelgård, J. Paatero, P. Lund, Impacts of time averaging on statistical analysis of photovoltaic generation, domestic electricity demand and grid voltages, Solar Energy 84 (2010) 492-500.

[18] H. Pihala, Non-intrusive appliance load monitoring system based on a modern kWh-meter, VTT Publications 356, Technical Research Centre of Finland, 1998.

[19] J.A. Duffie, W.A. Beckman, Solar Engineering of Thermal Processes, second ed., Wiley Interscience, New York, 1991.

[20] J.J. Grainger, W.D. Stevenson, Power System Analysis, McGraw-Hill, New York, 1994.

[21] MathWorks, MATLAB R2006a, http://www.mathworks.com/products/matlab/.

[22] J. Widén, Correlations between future wind and solar power generation in Sweden, Proceedings of the 3d International Conference on Energy Systems with IT, Älvsjö, Sweden, March 16-17, 2010.

[23] M. Bollen, P. Verde, A framework for regulation of rms voltage and short-duration under and overvoltages. IEEE Transactions on Power Delivery 23 (2008) 2105–2112.

[24] A. Svärd, Vattenfall Eldistribution AB, private communication.

Table 1: PV system model parameters.

Parameter	Value
μ	-0.004 [°C^{-1}]
$T_{c,STC}$	25 [°C]
I_{STC}	1000 [W/m^2]
$T_{c,NOCT}$	46 [°C]
$T_{a,NOCT}$	20 [°C]
I_{NOCT}	800 [W/m^2]
A_{ref}	1 [m^2]
P_{STC}	120 [W]
η_a	0.8

Table 2: Properties of the three LV grids.

Grid	Location	Main end-use category dimensioned for	Number of end-users
A	Urban area	Residential detached houses with district heating	181
B	Urban area	Residential detached houses with electric heating	107
C	Rural area	Residential detached houses with mixed types of heating	23

Table 3: Annual household electricity demand in the three LV grids.

Grid	Max [kWh/year]	Mean [kWh/year]	Min [kWh/year]
A	10277	4700	2315
B	8261	4559	2315
C	7852	4859	2320

Table 4: PV penetration level scenarios. All values are per household.

Peak power [kW]	PV array area A_c [m^2]	Annual production [kWh]
1	8.3	936
2	17	1872
3	25	2809
5	42	4681

Table 5: Average hours with PV production and reverse power flow through the MV/LV transformer substation. Results for grid A. Near-identical to results for the other grids.

Month	Mean hours with PV generation per day	Mean hours with reverse power flow per day		
		1 kW_p PV	2 kW_p PV	3 kW_p PV
1	8.0	0.2	0.8	1.2
2	9.8	0.9	2.7	3.2
3	12.6	1.2	2.3	2.8
4	15.3	2.0	4.9	6.1
5	18.1	3.2	6.8	8.6
6	19.8	3.4	6.8	8.9
7	18.9	3.5	7.1	8.8
8	16.5	2.6	6.0	7.2
9	13.7	2.0	4.5	5.5
10	11.0	0.9	2.5	3.1
11	8.7	0.4	1.8	2.2
12	7.4	0.1	0.8	1.1

Table 6: Network losses at different PV penetration levels.

Grid	Losses [kWh/year]			
	0 kW_p PV	1 kW_p PV	2 kW_p PV	3 kW_p PV
A	6254	5031	5546	7726
B	1730	1395	1548	2178
C	240	197	216	294

Table 7: Voltage spans in the three LV grids at different PV penetration levels.

PV [kW_p]	Voltage span [p.u.]		
	Grid A	Grid B	Grid C
0	0.976–1.000	0.987–1.000	0.988–1.000
1	0.976–1.007	0.987–1.003	0.988–1.002
2	0.976–1.022	0.987–1.011	0.988–1.006
3	0.976–1.036	0.987–1.018	0.988–1.011

Table 8: Total time with voltage in at least one household above the indicated level during the one-year simulation period. No households were affected at 1 kW_p PV per household.

Grid	Voltage level [p.u.]	Time [hours]	
		2 kW_p	3 kW_p
A	1.01	581	1093
	1.02	10	577
	1.03	0	115
B	1.01	8	552
	1.02	0	0
	1.03	0	0
C	1.01	0	25
	1.02	0	0
	1.03	0	0

Table 9: Percentage of households with voltage above the indicated level at least once during the one-year simulation period. No households were affected at 1 kW_p PV per household.

Grid	Voltage level [p.u.]	Households [%]	
		2 kW_p	3 kW_p
A	1.01	69	88
	1.02	10	54
	1.03	0	22
B	1.01	11	50
	1.02	0	0
	1.03	0	0
C	1.01	0	9
	1.02	0	0
	1.03	0	0

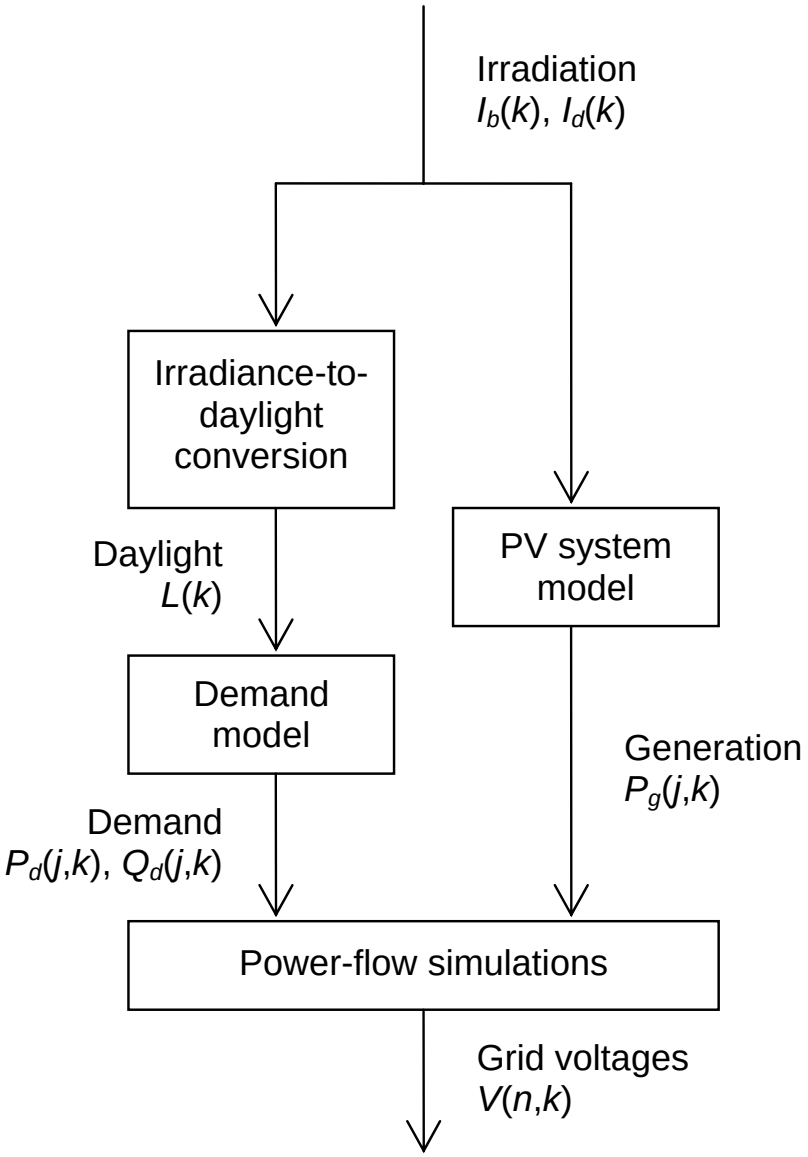

Figure 1: Flowchart showing the simulation procedure.

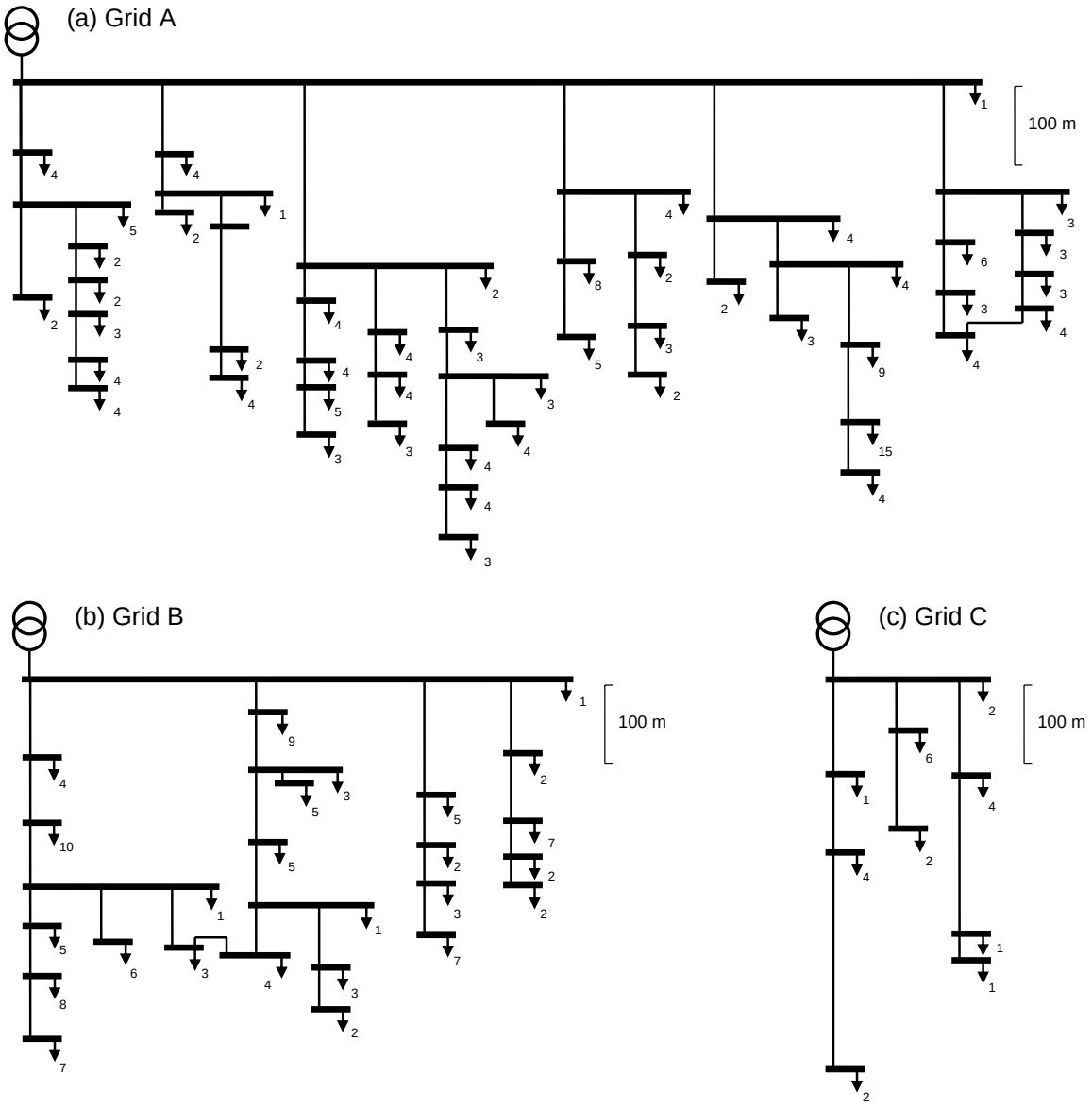

Figure 2: Schematic to-scale overview of the three LV grids. Cables from busbars to end-users are not shown but are indicated with arrows. The numbers show the number of end-users (households) connected to the busbars.

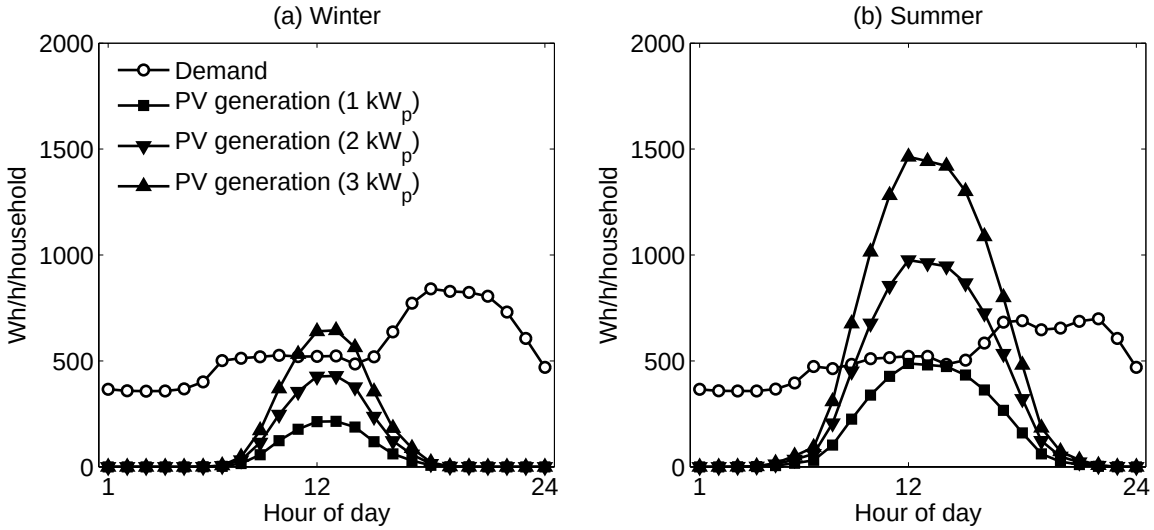

Figure 3: Mean daily demand and generation profiles with different penetration levels of PV for six-month winter (a) and summer (b) periods. The profiles are based on data for grid A, but are near-identical to those for the other grids. Summer period covers April through September and winter period covers October through March.

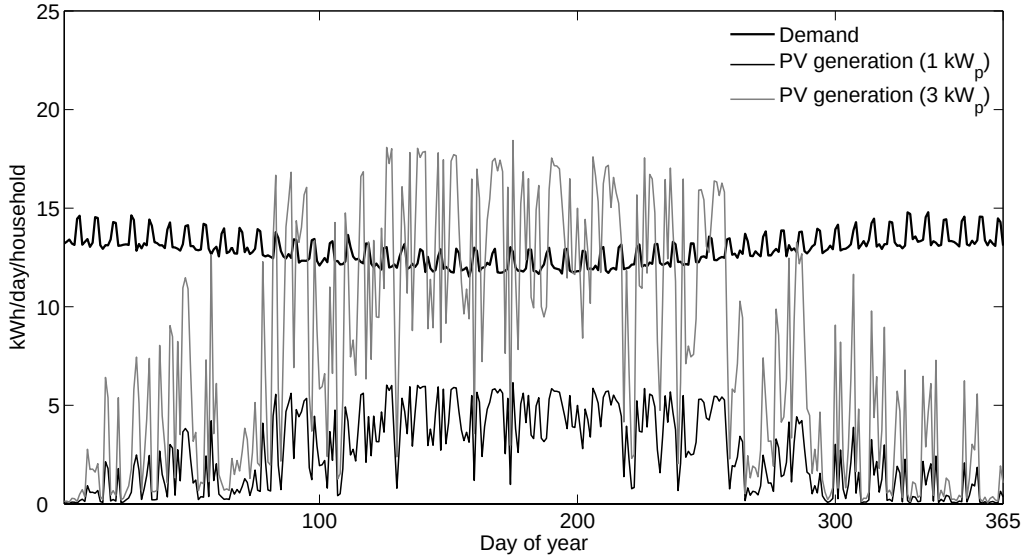

Figure 4: Annual distribution of daily demand and generation with two penetration levels of PV. The profiles are based on data for grid A, but are near-identical to those for the other grids.

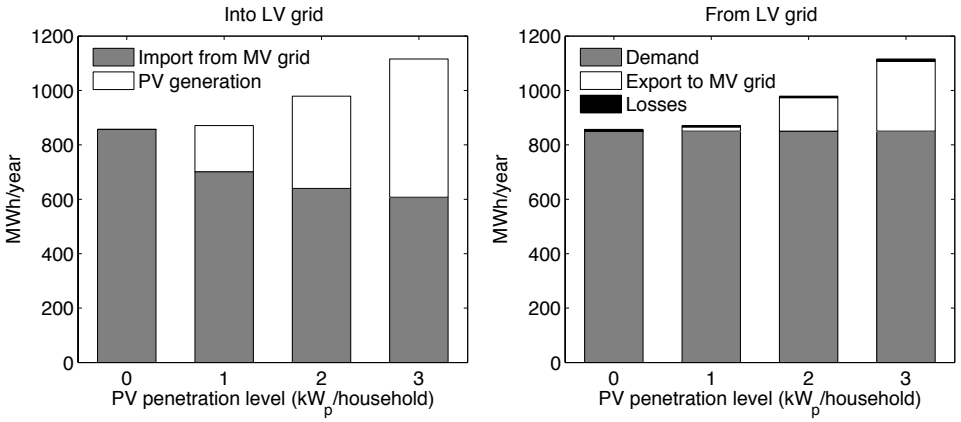

(a) Grid A

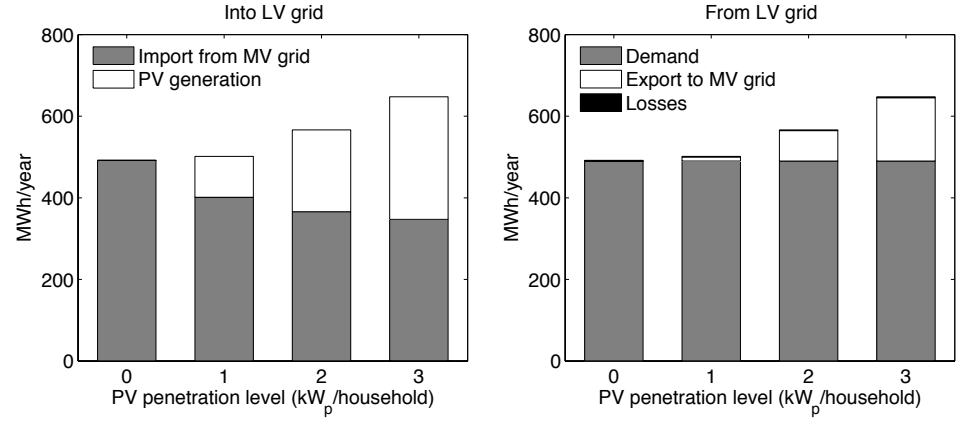

(b) Grid B

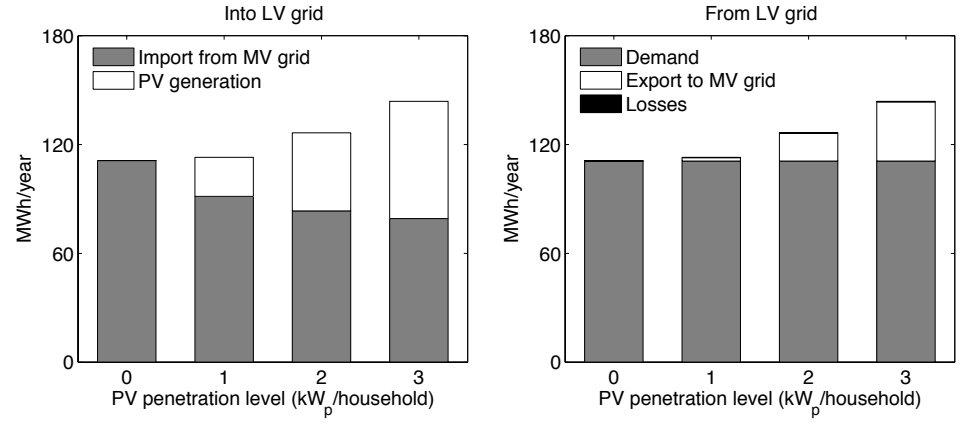

(c) Grid C

Figure 5: Annual aggregated energy injected into and extracted from the LV grids at different PV penetration levels.

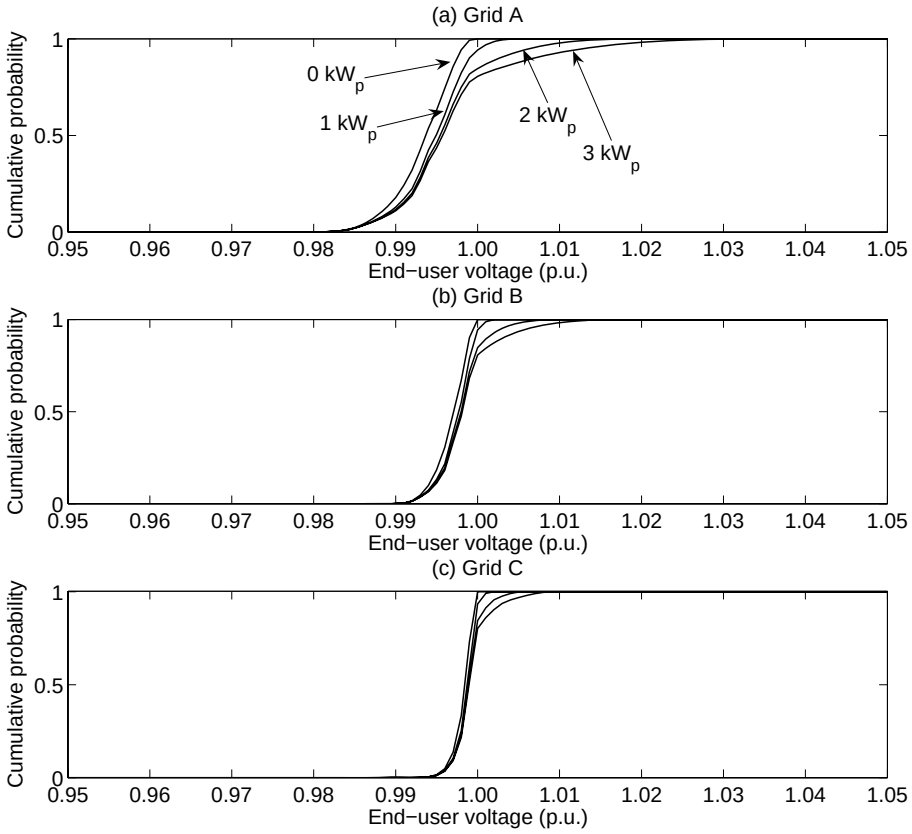

Figure 6: Cumulative probability for end-user voltages calculated over all household nodes in the three LV grids. The mutual order of scenarios in the two lower graphs is the same as in the upper figure.

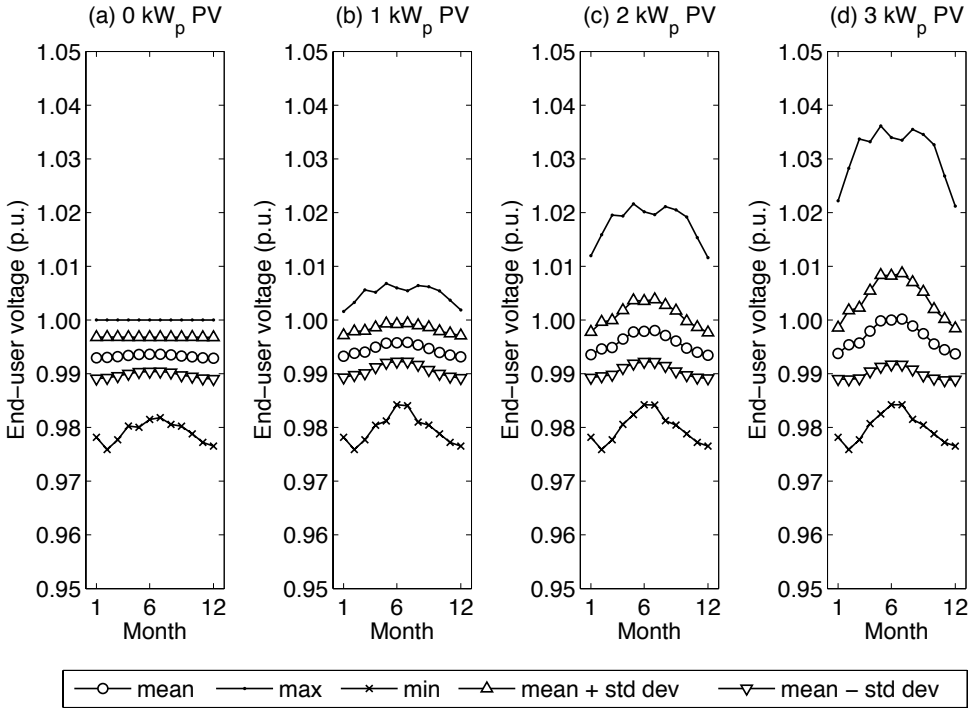

Figure 7: Monthly variation of end-user voltages in grid A at different PV penetration levels.

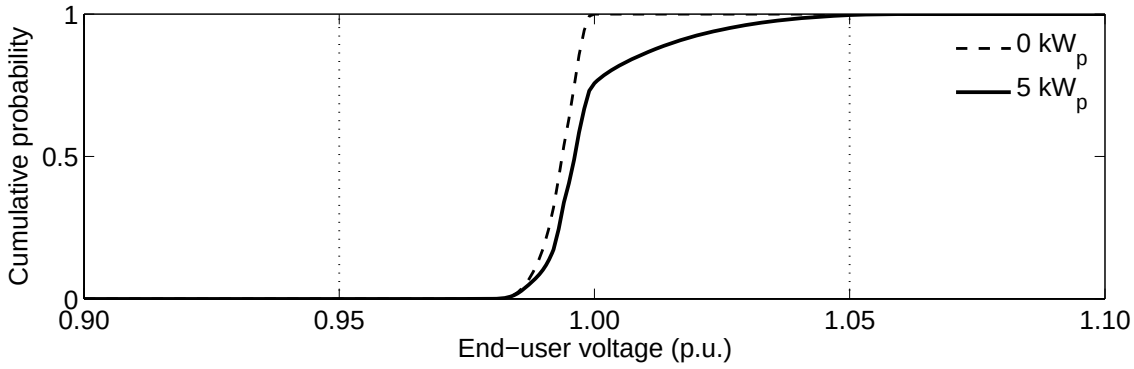

Figure 8: Cumulative probability for end-user voltages calculated over all household nodes in grid A without PV (0 kW_p) and with zero-energy houses (5 kW_p).

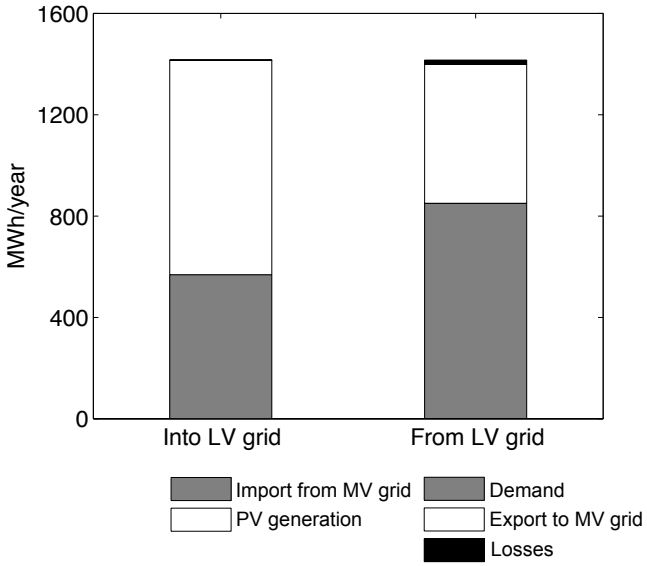

Figure 9: Annual aggregated energy injected into and extracted from grid A with zero-energy houses (5 kW_p PV per household).